I&EC research
Industrial & Engineering Chemistry Research

Article

pubs.acs.org/IECR

Colloidal Processing of $Mg(OH)_2$ Aqueous Suspensions Using Sodium Polyacrylate as Dispersant

Kefeng Tong,[†] Xingfu Song,*[,†] Guoping Xiao,[‡] and Jianguo Yu*[,†]

[†]National Engineering Research Center for Integrated Utilization of Salt Lake Resources, East China University of Science and Technology, Shanghai 200237, China

[‡]Shanghai Institute of Applied Physics, Chinese Academy of Science, Shanghai 201800, China

ABSTRACT: The rheological behavior and stability of $Mg(OH)_2$ suspensions were studied in the presence of sodium polyacrylate with different molecular weights under conditions of different ionic strength and counterion valence (K^+ and Mg^{2+}). Rheological properties, optical absorbance, and zeta potential measurements were conducted on the $Mg(OH)_2$ particle suspensions to assess the dispersing ability of the sodium polyacrylate dispersants. Adsorption isotherm measurements were applied to investigate the effect of counterions on the adsorption behavior. The results demonstrate that Mg^{2+} ions destabilize the $Mg(OH)_2$ suspensions more dramatically than K^+ ions due to the stronger screening effect and special complexation of Mg^{2+} ions and carboxyl groups. The effect of molecular weights of NaPA on the rheological properties becomes more pronounced at higher solid loading because the NaPA with a molecular weight of 15,000 g/mol increases the viscosity more obviously than NaPA with a molecular weight of 1200 g/mol. The calculation results of interparticle interaction by the Hamaker 2 program show that the suspensions can achieve good stability with sufficient NaPA dosage, which coincides with the optical absorbance measurement results.

1. INTRODUCTION

Magnesium hydroxide has attracted much attention over years owing to its wide applications in the environmental fields,[1−3] as well as pharmaceutical productions.[4−6] Magnesium hydroxide in the form of suspension is preferable than those in the forms of powder and filter cake due to its advantages of being expediently handled, stored, transported, and pumped.[7] Additionally, the solid loading of magnesium hydroxide suspensions can be flexibly regulated according to the applying conditions. However, magnesium hydroxide particles will easily settle and agglomerate in the aqueous medium because the particles are hydrophilic[8] and have high surface energy,[9] which leads to an increase in viscosity of suspensions. Hence, a technological crux should be emphasized on the preparation methods of magnesium hydroxide suspensions with adequate fluidity and sufficient stability against aggregation and sedimentation of particles over a broad range of solid loading.

It is well known that low molecular weight polyelectrolytes are frequently used as additives to regulate the rheological properties and stability of concentrated particulate suspensions, thus facilitating many industrial processes.[7,10,11] When adsorbed onto the surfaces of solid particles, these polyelectrolytes can provide effective electrostatic repulsion by the charged segments or steric repulsion by the adsorbed layers to counteract the interparticle attractions. However, the adsorbed conformations of polyelectrolytes are complex depending on the pH and ionic strength of solvent medium,[12−15] as well as the molecular weights of polyelectrolytes, eventually leading to a variation in the stability of suspensions. When the polyelectrolytes adsorb flatly onto the surfaces, the stabilization mechanism mainly results from electrostatic interaction. This electrostatic interaction may be greatly affected by the salts species in the solution because of the screening effect of salts on the charged polyelectrolyte segments and surface charges. With increasing the thickness of adsorbed layers, the contribution of steric repulsion is in charge of the stabilization for the suspensions.[16,17]

Additionally, the selection of molecular weights and dosage of polyelectrolytes should be deliberate according to the preparing conditions such as solid loading, particle size, etc. Polyelectrolytes may induce flocculations either by a particle-binding bridge via the simultaneous adsorption of polyelectrolyte on two or more neighboring surfaces when the molecular weight is high or by the depletion effect of nonadsorbed polyelectrolytes when their molecular weights are larger or comparable in size to the particles in the suspensions.[18,19]

In this study, sodium polyacrylate was used as the dispersant for $Mg(OH)_2$ suspensions. The effects of molecular weights, ionic strength, and counterion valence on the rheological behavior and stability of $Mg(OH)_2$ suspensions were evaluated via the rheological properties, optical absorbance, adsorption isotherm, and zeta potential measurements. The interparticle interactions in suspensions were calculated using Hamaker 2 program[20] as a validation of experimental results.

2. EXPERIMENTAL METHODS

2.1. Materials. Commercially available $Mg(OH)_2$ powder (purity of 99%, No.4 Reagent, H.V. Chemical Co., Ltd., Shanghai) was used as the raw material. The anionic polyelectrolytes, sodium polyacrylate (Sigma-Aldrich) with

Received: January 21, 2014
Revised: February 24, 2014
Accepted: March 5, 2014
Published: March 5, 2014

dx.doi.org/10.1021/ie5002857 | *Ind. Eng. Chem. Res.* 2014, 53, 4755−4762

weight-average molecular weights of 1200 and 15,000 g/mol, were used as the dispersants in this study, which were denoted as NaPA (1200) and NaPA (15,000), respectively. Due to the high pH value and strong buffer ability of $Mg(OH)_2$ suspensions, the COOH groups on the backbone of sodium polyacrylate are supposed to be fully deprotonated throughout the experiments, with an equal amount of Na^+ ions to maintain the systems electrically neutral.

2.2. Rheological Measurements. The aqueous $Mg(OH)_2$ suspensions of varying solid loading were prepared with various amounts of NaPA, dispersed by an emulsifier (BME 100 LX, Weiyu Mechano-electronic Manufacturing Co., Ltd., Shanghai) at 3000 rpm for 20 min, and then the mixtures were allowed to stand for 24 h. The viscosity measurements were performed by employing a Bolin CVO rheometer (Malvern Instruments) fitted with a concentric cylinder geometry. In order to break up any possible flocs and ensure reproducibility of the data, the suspensions were presheared at a shear rate of 200 s^{-1} for 1 min and were left standing for an additional 1 min prior to each measurement. The important influences of solid loading, ionic strength (adjusted by KNO_3 and $MgCl_2$), dosage, and molecular weights of polyelectrolyte dispersants were investigated during the measurements.

2.3. Stability Measurements. The stability of the $Mg(OH)_2$ aqueous suspensions was estimated from the variation of the optical absorbance of suspensions using an UV/vis spectrophotometry (Shimadzu uv-2550). For the stability measurements, a series of 100 mL suspensions with 0.2 g $Mg(OH)_2$ particles were prepared, and a 10 mL solution with a given amount of NaPA was added to these 100 mL suspensions. The mixtures were ultrasonicated for 30 min and left stirred for another 24 h at room temperature. Then the suspensions were poured into a glass cuvette, and the dependence of absorbance on sedimentation time was recorded at λ = 590 nm. The absorbance of the well-stabilized suspension is higher relative to the smaller sedimentation rate.

2.4. Adsorption Isotherm Measurements. Adsorption isotherm measurements were carried out by agitating the suspensions with 5 wt % $Mg(OH)_2$ powder and various concentrations of NaPA at 100 rpm for 24 h. During the adsorption process, pH adjustment was not performed because the suspensions had an almost stable pH value ($\sim$ 11.5) at any NaPA concentrations. After equilibrium, the suspensions were centrifuged at 5000 rpm for 20 min, and the supernatants were withdrawn to detect the residual NaPA concentration using a Liqui TOC analyzer (Elementar Germany). The amount of NaPA adsorbed on the surface of $Mg(OH)_2$ particles was determined by calculating the difference between the NaPA concentration in stock solution and that in the supernatant.

2.5. Zeta Potential Measurements. In order to study the possible electrostatic stabilization and influence of NaPA on the charges of particle surface, a zeta potential meter (JS94H2, Zhongchen Powereach Co., Ltd., Shanghai) was used for measuring zeta potentials of $Mg(OH)_2$ suspensions. The preparation of suspensions for zeta potential measurements is similar to that for stability measurements except the addition of 0.001 M NaCl salts as the background electrolyte. After a 24 h rest, the supernatants were taken, and the zeta potential of the remaining powders in the supernatants was measured as a function of NaPA concentration. Each measurement was repeated at least 10 times to eradicate any discrepancies.

2.6. Interparticle Potential Calculation. The interparticle interactions were calculated by a freeware Hamaker 2 program[20] to evaluate the stability of suspensions. This program predicts the interactions within the DLVO model by adding the steric interaction model, in which the total interparticle potential, V_{total}, is described as follows

$$V_{total} = V_{vdW} + V_{elec} + V_{steric} \tag{1}$$

where V_{vdW}, V_{elec}, and V_{steric} belong to the contributions of the attractive van der Waals interactions, electrostatic interaction, and steric interactions, respectively.

2.6.1. van der Waals Interactions. In this system, V_{vdW} can be calculated according to the Hamaker model, as shown in eq 2

$$V_{vdW} = \frac{A}{6}\left[\frac{2a_1a_2}{h^2 + 2a_1h + 2a_2h} + \frac{2a_1a_2}{h^2 + 2a_1h + 2a_2h + 4a_1a_2} + \ln\left(\frac{h^2 + 2a_1h + 2a_2h}{h^2 + 2a_1h + 2a_2h + 4a_1a_2}\right)\right] \tag{2}$$

where A is the effective Hamaker constant for the studied system, h is the particle surface−surface minimum separation, and a_1 and a_2 are the radii of particles. For this system, $a_1 = a_2$ because there are only $Mg(OH)_2$ particles.

2.6.2. Electrostatic Interactions. When the suspensions consist of particles with charged surfaces, the diffuse double layers of the two particles begin to interfere with each other as they approach each other from infinity, leading to an increase in free energy.[21] This change in free energy, as $V_{electrostat}$, can be calculated by the widely used HHF expression[22]

$$V_{HHF}(h) = \frac{\pi\varepsilon\varepsilon_0 a_1 a_2}{a_1 + a_2}\left[(\psi_1 + \psi_2)^2\ln(1 + \exp(-\kappa h)) + (\psi_1 - \psi_2)^2\ln(1 - \exp(-\kappa h))\right] \tag{3}$$

where ε and ε_0 are the dielectric constant and electric constant, respectively, and ψ is the surface potential, which can be calculated from the experimentally accessible zeta potential as given by eq 4

$$\psi = \zeta\exp(\kappa d_s) \tag{4}$$

where ζ is the experimentally measured zeta potential, d_s is the distance from the surface where the zeta potential is measured, and the reciprocal of κ is Debye length (κ^{-1}), which can be calculated through a combination of eqs 5 and 6

$$I_c = \frac{1}{2}\sum c_i z_i^2 \tag{5}$$

$$\kappa^{-1} = \sqrt{\frac{\varepsilon_0\varepsilon kT}{2e^2 I_c 1000 N_A}} \tag{6}$$

where I_c is the ionic strength in solution medium, c_i is the molar concentration of ionic species i with a valence z_i, e is the elementary charge, and N_A is the Avogadro's constant.

2.6.3. Steric Interactions. The hard-wall model introduced by Bergström was implemented for the steric interaction calculations. According to the relationship of interparticle distance h and adsorbed layer thickness d_a, the interaction potential for the hard-wall model can be divided into three domains. The interaction potentials are infinitely repulsive and constantly zero when $h < d_a$ and $h > 2d_a$, respectively. As the

dx.doi.org/10.1021/ie5002857 | Ind. Eng. Chem. Res. 2014, 53, 4755−4762

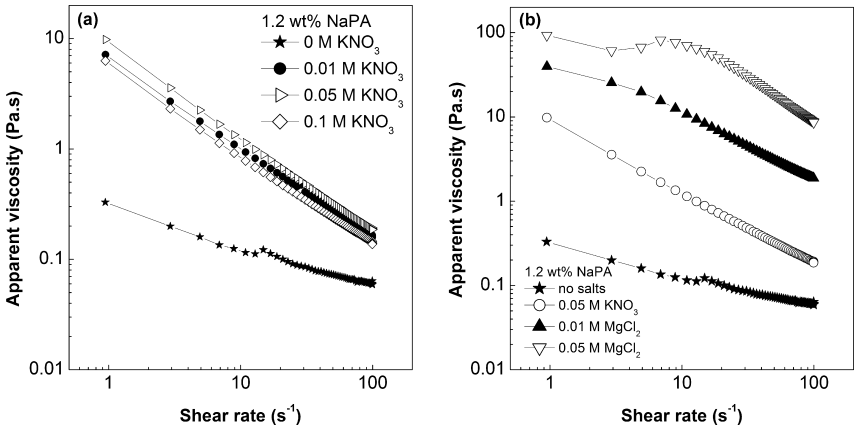

Figure 1. Effect of ionic strength on the rheological behavior of 40 wt % $Mg(OH)_2$ suspensions: molecular weight of NaPA, 1200 g/mol; NaPA dosage, 1.2 wt %. (a) Monovalent K^+ ions. (b) Valence of metal ions (K^+ and Mg^{2+}).

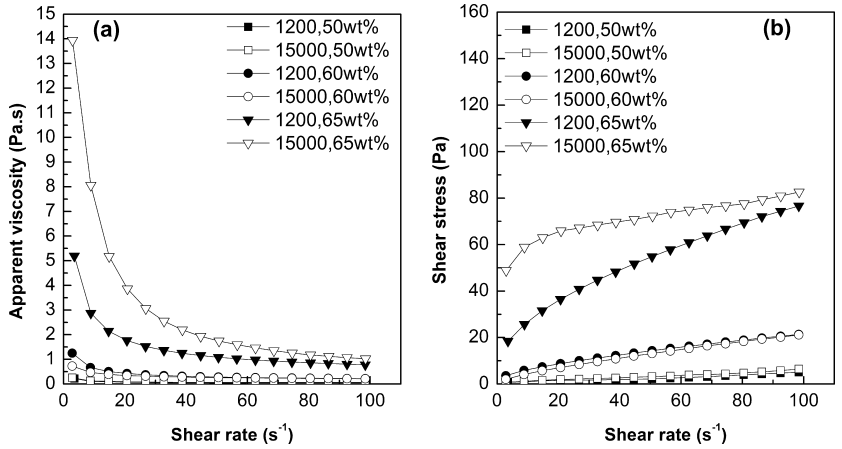

Figure 2. Effect of molecular weights on the rheological behavior of $Mg(OH)_2$ suspensions as a function of solid loading: dosage of NaPA: 1 wt % (based on the $Mg(OH)_2$ powder). (a) Apparent viscosity. (b) Shear stress.

interpenetrated domain is within a separation of twice the adsorbed layer thickness, corresponding to the domain $d_a \leq h \leq 2d_a$, the steric interaction potential V_{steric} is given by

$$V_{steric} = \frac{\pi akT}{V\varphi^2}\left(\frac{1}{2} - \chi\right)(2d_a - h)^2 \quad (7)$$

where a is the particle radius, V is the molecular volume of the solvent, φ is the volume fraction of molecules in the adsorbed layer, and χ is the molecule-solvent interaction.

3. RESULTS AND DISCUSSION

3.1. Rheological Behavior. The ionic strength can significantly affect the stabilization of the suspensions by changing the thickness of the electrical double layer in electrostatic stabilization[18,23] and also collapsing the extend polyelectrolyte layer in electrosteric stabilization.[24,25] Hence, the effects of ionic strength and counterion valence on the rheological behavior of $Mg(OH)_2$ suspensions were investigated. The apparent viscosity of 40 wt % $Mg(OH)_2$ suspensions with 1.2 wt % of NaPA (based on the $Mg(OH)_2$ powder) were measured at a shear rate range of 1−100 s^{-1}, as depicted in Figure 1. The ionic strength was varied by the addition of monovalent (KNO_3) or divalent ($MgCl_2$) salts species. Figure 1(a) illustrates the variation of apparent viscosity of $Mg(OH)_2$ suspensions with KNO_3 concentration. Over the applied KNO_3 concentration, the flow curves of suspensions are almost Newtonian with slight shear thinning behaviors. It indicates that sufficient NaPA dosage may impart effective electrosteric stabilization to the concentrated $Mg(OH)_2$ suspensions to weaken the adverse effect of KNO_3 on fluidity. However, as shown in Figure 1(b), the apparent viscosity increases more pronouncedly in the presence of divalent ion Mg^{2+} compared to monovalent ion K^+. In the suspension containing 0.05 mol/L $MgCl_2$, a viscosity plateau is obtained before the shear rate of approximately 10 s^{-1}, corresponding to the abundant flocs in the concentrated suspension. This is because that Mg^{2+} ions effectively screen the negative charges of NaPA[26] and may bind to the carboxyl groups to form polyelectrolyte−Mg^{2+} complexes,[27] and particle flocculation usually ensues under such conditions. Additionally, the solubility of complexes may decrease to form precipitates as Mg^{2+} concentration increases, resulting in reduction of the actual concentration of NaPA. Therefore, the dispersing ability of NaPA is worse in the $Mg(OH)_2$ suspensions with Mg^{2+} ions in comparison to K^+ ions.

Figure 2 shows the effect of NaPA molecular weights on the rheological behavior of the suspensions as a function of solid loading. One wt % NaPA with molecular weights of 1200 and 15,000 g/mol were added to the suspensions. In the suspensions with 50 wt % $Mg(OH)_2$ powder, the flow curves exhibit almost Newtonian flow with both NaPA (1200) and NaPA (15,000), corresponding to the well-stabilized suspen-

dx.doi.org/10.1021/ie5002857 | Ind. Eng. Chem. Res. 2014, 53, 4755−4762

sions, while in the 60 wt % suspensions, the flow curves show weak shear thinning behavior as shear rate increases and the apparent viscosity increases compared to that in the 50 wt % suspensions at the corresponding shear rate. At the solid loading of 65 wt %, the suspensions show more evident shear thinning behaviors with relatively higher apparent viscosity in comparison with the suspensions with 50 and 60 wt % solid loading. In addition, the effect of molecular weights of NaPA on the rheological properties becomes more pronounced at the solid loading of 65 wt % as depicted in Figure 2(b). As shear rate increases, a larger shear stress is observed to break the flocs in the suspensions with NaPA (15,000) than that with NaPA (1200). Two factors may be contributing to the formation of flocs and increasing apparent viscosity in the high concentrated suspensions as following. First, the interparticle distance reduces as the solid loading increases, leading to a more pronounced influence from the long-range van der Waals attraction.[28−30] This reduction of interparticle distance may also lead to the compression of electric double layers of particles, which impairs the electrostatic repulsion.[31] Second, the adsorption layer of the polyelectrolyte can be added to the volume fraction of solid particle to yield an effective volume fraction[18,32] as following

$$\phi_{\text{eff}} = \phi\left(1 + \frac{\delta}{R}\right)^3 \tag{8}$$

where ϕ_{eff} is the effective volume fraction, δ is the adsorption layer thickness of polyelectrolyte, and R is the radius of particles. When in the suspensions with higher solid loading, the effective volume fraction increases significantly with molecular weight of dispersant, especially in the systems of nanoparticles. Therefore, the effective volume fraction can be considerably higher than the nominal one, thus leading to a high apparent viscosity. In addition, the depletion flocculation probably occurs because the nonadsorbed polyelectrolyte molecules may be comparable in size to the interparticle distance in the suspensions with higher solid loading.[13,18,19,33]

Due to the flocs in the concentrated suspensions, an applied stress exceeding a certain critical level, i.e., the yield stress (τ_y), which is dependent on the interparticle forces, volume fraction, particle size, and size distribution,[34,35] is needed to break the flocs and fluidify the particulate suspensions.[36] Hence, the Herschel−Bulkley model was used to fit the shear stress−shear rate curves in Figure 2(b) and estimate the yield stress τ_y[37]

Herschel−Bulkley model:

$$\tau = \tau_y + K\gamma^n \tag{9}$$

where τ_y is the yield stress determined from the Herschel−Bulkley model, η_s is the model intrinsic viscosity, K is a viscosity coefficient, and n is the shear rate exponent. As shown in Table 1, the correlation coefficients for the Herschel−Bulkley model are higher than 0.98 over the applied experimental conditions, suggesting excellent fitting capability of the Herschel−Bulkley model in our systems. It is evident that the yield stress increases with solid loading, and this increase becomes more distinct as solid loading increases above 60 wt %. Furthermore, the addition of NaPA with larger molecular weight appears to result in a higher yield stress in the suspensions of 65 wt % solid loading, suggesting a more drastic flocculation.[38] Hence, the fitting results coincide with the evolution of rheological behavior of $Mg(OH)_2$ suspensions under the applied conditions in Figure 2, and the variation of yield stress is useful in evaluation in the degree of flocculation.[39]

Table 1. Yield Stress of $Mg(OH)_2$ Suspensions Determined from Herschel−Bulkley Model[a]

	yield stress of suspensions, τ_y (Pa)	
solid loading (wt %)	molecular weight (1200)	molecular weight (15,000)
50	1.0188 (0.9884)	0.6201 (0.9877)
60	1.8111 (0.9999)	0.9129 (0.9999)
65	8.5039 (0.9999)	16.3308 (0.9885)

[a]Data in parentheses are the correlation coefficients.

3.2. Stability Measurements. The influences of NaPA molecular weights and counterions on the stability of a $Mg(OH)_2$ aqueous suspension were investigated via optical absorbance tests using UV/vis spectrophotometry. Figure 3 illustrates the absorbance of $Mg(OH)_2$ suspensions for two molecular weights of NaPA as a function of sedimentation time. In these tests, 10 mL of 200 ppm NaPA solution was added to each 100 mL of 2 g/L $Mg(OH)_2$ suspension, in which the ionic strength was adjusted by KNO_3 or $MgCl_2$. As shown in Figure 3, all the absorbance of $Mg(OH)_2$ suspensions tends to decrease as the sedimentation proceeds. However, the decreasing rate of absorbance is significantly susceptible to the molecular weights and counterions valence. Because the carboxylic groups are almost fully dissociated in the basic $Mg(OH)_2$ suspensions, the NaPA chains adopt an extended coil configuration due to the electrostatic repulsion between adjacent highly charged carboxylic segments.[40] Hence, these polyelectrolyte chains would adsorb onto the particle surface in the formation of open coils and thick adsorption layer,[17,33] providing an effective electrosteric repulsion that induces stability. In addition, the adsorbed NaPA chains of higher molecular weight (15,000) induce stronger steric stabilization compared to that of their lower molecular weight counterpart (1200).[16,41] Therefore, the suspensions in the presence of NaPA (15,000) achieve better stability than the suspension with NaPA (1200) without the addition of a salts species.

From Figure 3, the addition of counterions (K^+ and Mg^{2+}) changes the decreasing rate of absorbance distinctly. The steep reduction of absorbance in the 0.01 M KNO_3 solution reflects the appearance of evident flocculation due to the detrimental influence of excess K^+ ions on the dispersing ability of NaPA. Furthermore, it is observed that the absorbance decreases at a faster rate in a 0.001 M $MgCl_2$ solution compared to KNO_3 in the same molar concentration, suggesting a stronger destabilizing effect of Mg^{2+} than K^+. This may be contributed to the stronger screen effect of Mg^{2+} on the negative charges of NaPA than K^+ and the complexation interaction of Mg^{2+} and the carboxyl groups.[27]

3.3. Adsorption Isotherm. Figure 4 shows the NaPA adsorption isotherm of $Mg(OH)_2$ suspension with 5 wt % solid loading. The applied NaPA polyelectrolytes have molecular weights of 1200 and 15,000 g/mol, and the ionic strength of $Mg(OH)_2$ suspensions was adjusted by 0.001 M $MgCl_2$ or KNO_3 solutions. The adsorbed amount of NaPA increases with the initial NaPA dosage without any equilibrium in the adsorptions of both NaPA polyelectrolytes. A possible explanation for this high adsorption of NaPA in $Mg(OH)_2$ suspensions is given as follows. Because the pH value of $Mg(OH)_2$ suspensions is maintained to be about 11.5 in the systems, which is slightly less than the pH_{IEP} values of the studied systems (pH_{IEP} values are 11.9 for the salt-free system,

dx.doi.org/10.1021/ie5002857 | Ind. Eng. Chem. Res. 2014, 53, 4755−4762

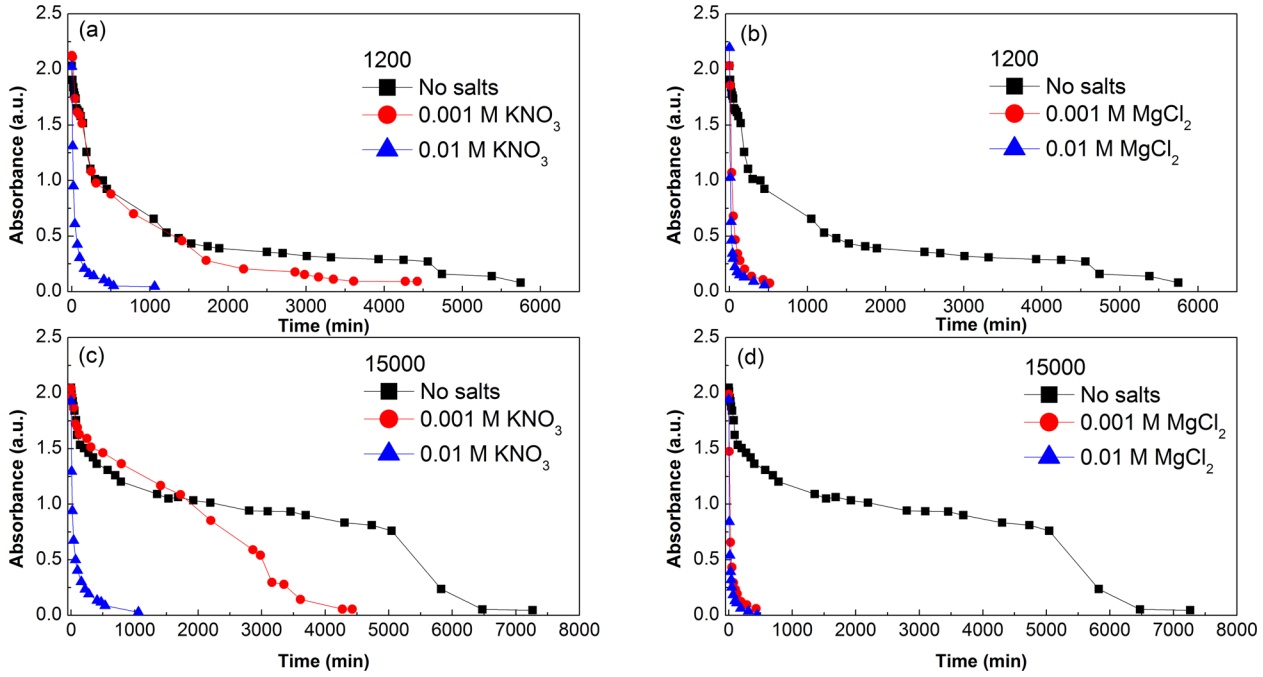

Figure 3. Effect of NaPA molecular weight and ionic strength on the absorbance of $Mg(OH)_2$ suspensions. (a) and (b): NaPA (1200). (c) and (d): NaPA (15,000).

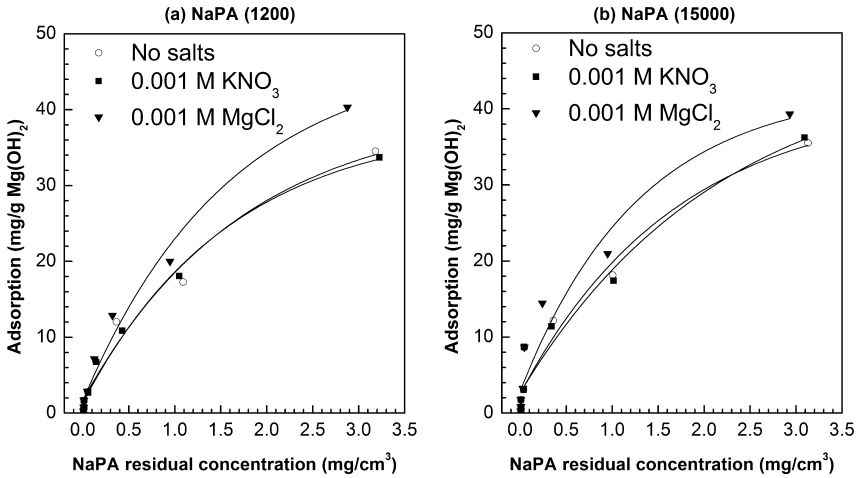

Figure 4. NaPA adsorption isotherm of $Mg(OH)_2$ suspensions with 5 wt % solid loading. (a) NaPA (1200). (b) NaPA (15,000).

11.9 for the system with 0.001 M KNO_3, and 12.2 for the system with 0.001 M $MgCl_2$, which are similar to the reported pH_{IEP} of 12[42]), electrostatic interaction of negatively charged polyelectrolyte and positively charged sites of $Mg(OH)_2$ particle surfaces may take place.[43] Additionally, a strong binding interaction between ionized carboxyl groups and surface Mg^{2+} ions may also lead to an irreversible high adsorption.

As also shown in Figure 4, the adsorption amount of NaPA increases evidently with the addition of $MgCl_2$ electrolytes, whereas the adsorption amount of NaPA does not increase in the KNO_3 solution. This is because the special interaction between Mg^{2+} ions and carboxyl groups strongly promotes the adsorption behavior of NaPA in several ways: (1) The screening effect of Mg^{2+} ions on the charged carboxyl groups reduces intra/intersegment repulsion, leading to a denser adsorption layer with large adsorption amount. (2) The solubility of NaPA will be reduced due to the complexation of Mg^{2+} and carboxyl groups,[27] corresponding to an increase in adsorption of NaPA. (3) The possible intersegment bridges between carboxyl groups linked by Mg^{2+} ions ($R\text{-}COO^{-}-Mg^{2+}-{}^{-}OOC-R$) is also beneficial for the adsorption of NaPA.[43−46]

3.4. Zeta Potential. The changes in surface charge of $Mg(OH)_2$ particle as a function of NaPA addition are illustrated by zeta potential measurements in Figure 5. It is shown that the changes in zeta potential are almost identical for NaPA (1200) and NaPA (15,000). The addition of both NaPA polyelectrolytes increases the negative surface charges until a nearly plateau at about −20 mV is reached. The addition of NaPA not only increases adsorption amount but also the adsorption layer thickness. The thicker adsorption layer indicates that the shear plane may shift to a greater distance from the particle surface, leading to a reduction in the magnitude of the zeta potential.[47] Hence, the negative zeta potential no longer increases, regardless of the negative charge

dx.doi.org/10.1021/ie5002857 | Ind. Eng. Chem. Res. 2014, 53, 4755−4762

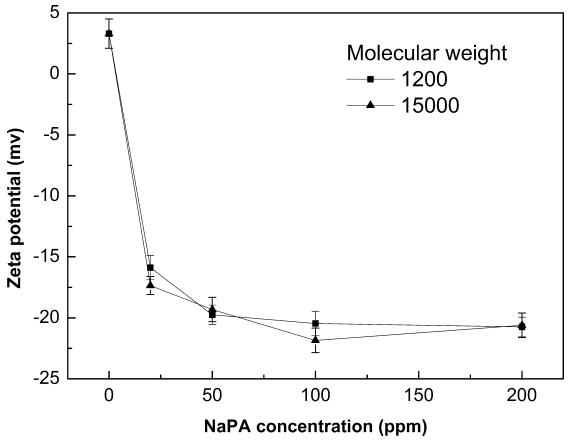

Figure 5. Zeta potential of $Mg(OH)_2$ suspensions at various NaPA concentrations.

accumulation stemming from an increase in adsorption of ionized polyelectrolytes.

3.5. Interparticle Potential Calculation. Interparticle interactions between particles were calculated to assess the stability of the $Mg(OH)_2$ suspensions with a freeware Hamaker 2 Program.[20] The Hamaker constant A can be calculated as follows

$$A = (3/4)\kappa T\left(\frac{\varepsilon_p - \varepsilon_m}{\varepsilon_p + \varepsilon_m}\right)^2 + \frac{3\hbar\omega(n_p^2 - n_m^2)^2}{16\sqrt{2}(n_p^2 + n_m^2)^{3/2}} \quad (10)$$

where κ is Boltzmann's constant, $\kappa = 1.38 \times 10^{-23}$ J/K, T is the absolute temperature, $T = 298$ K, $\hbar$ is Planck constant, $\hbar = 6.63 \times 10^{-34}$ J s, ω is the UV adsorptive frequency, $\omega = 3.0 \times 10^{15}$ s^{-1}, ε_p and ε_m are the dielectric constants of particles and water medium, respectively, $\varepsilon_p = 2.87$ F/m and $\varepsilon_m = 78.36$ F/m, n_p and n_m are the index of refraction of particles and water medium, respectively, and $n_p = 1.56$ and $n_m = 1.33$. According to eq 10, the Hamaker constant of $Mg(OH)_2$ particles was calculated to be 1.62×10^{-20} J. Table 2 lists the data used for interparticle interaction calculations.

The interparticle potential calculation results for $Mg(OH)_2$ suspensions as a function of NaPA dosage are shown in Figure 6. It can be found that the $Mg(OH)_2$ suspensions without NaPA dispersants have attractive potentials in all the interparticle distances, suggesting that the agglomeration of $Mg(OH)_2$ particles would occur and that the suspensions are not stable. Increasing the NaPA dosage will improve the stability of $Mg(OH)_2$ suspensions. The interparticle potentials in the suspensions with 10 mL NaPA solutions of 20 and 50 ppm are dependent on interparticle distance. $Mg(OH)_2$ particles in the interparticle distance above about 2 nm are mutually repulsive. However, $Mg(OH)_2$ particles are attractive to each other in the interparticle distance below 2 nm, while the suspensions with 10 mL NaPA solutions of 100 and 200 ppm have repulsive potentials corresponding to the stable suspensions. These interparticle potential calculation results coincide with the stability measurements, indicating that sufficient NaPA dosage can impart stability to the $Mg(OH)_2$ suspensions.

4. CONCLUSIONS

In this paper, the rheological properties and stability of $Mg(OH)_2$ aqueous suspensions were investigated using sodium polyacrylate (NaPA) as the dispersant. Two NaPA polyelectrolytes with different molecular weights were selected. The effects of ionic strength and counterion valence on the rheological behavior and adsorption isotherm of $Mg(OH)_2$ suspensions were also studied. It can be found in the rheological properties and absorbance measurements that Mg^{2+} ions impart a stronger destabilizing effect to the $Mg(OH)_2$ suspensions than K^+ ions because of the screening effect and special complexation of Mg^{2+} ions and carboxyl groups. The special complexation between Mg^{2+} and carboxyl groups can also promote the adsorption of NaPA onto the surfaces of $Mg(OH)_2$ particles as described in the Adsorption Isotherm section. The difference in viscosity of $Mg(OH)_2$ suspensions, originating from the different molecular weights of NaPA, becomes much more pronounced as the solid loading increases to 65 wt %. Compared to the NaPA with a molecular weight of 1200 g/mol, a more evident shear thinning behavior is observed in the $Mg(OH)_2$ suspensions in the presence of NaPA with a molecular weight of 15,000 g/mol, indicating a more serious flocculation. In conclusion, according to the rheological experiments, 1.2 wt % NaPA with a molecular weight of 1200 g/mol can successfully induce sufficient stabilization and effectively reduce the viscosity of the 40 wt % $Mg(OH)_2$ suspensions without the addition of salt electrolytes in the studied systems, and the destabilizing effect of the applied K^+ ions concentrations on the $Mg(OH)_2$ suspensions is much less significant compared to the applied Mg^{2+} ions concentrations. The interparticle potential results calculated by Hamaker 2 program are quite consistent with the experimental results in absorbance measurements, which confirmed that sufficient NaPA dosage can provide the $Mg(OH)_2$ particles with repulsive potentials and consequently stabilize the particulate suspensions.

Table 2. Data Used for Interparticle Interaction Calculations

molecular weights of NaPA (g/mol)	dosage of NaPA (ppm)	pH value	zeta potential (mv)	charge plane (nm)	ionic strength (mol/L)	particle density (g/cm^3)	particle diameter* (Dv50) (μm)	Hamaker constant ($\times 10^{-20}$ J)
1200	20	11.5	−15.88	0.1	0.001	2.36	1.943	1.62
	50	11.5	−19.75	0.5	0.001	2.36	1.727	1.62
	100	11.5	−20.46	1	0.001	2.36	1.571	1.62
	200	11.5	−20.74	2	0.001	2.36	1.398	1.62
15,000	20	11.5	−17.35	0.1	0.001	2.36	2.318	1.62
	50	11.5	−19.32	0.5	0.001	2.36	2.103	1.62
	100	11.5	−21.85	1	0.001	2.36	2.011	1.62
	200	11.5	−20.61	2	0.001	2.36	1.945	1.62

*Particle diameters were measured by a Malvern mastersizer.

dx.doi.org/10.1021/ie5002857 | Ind. Eng. Chem. Res. 2014, 53, 4755−4762

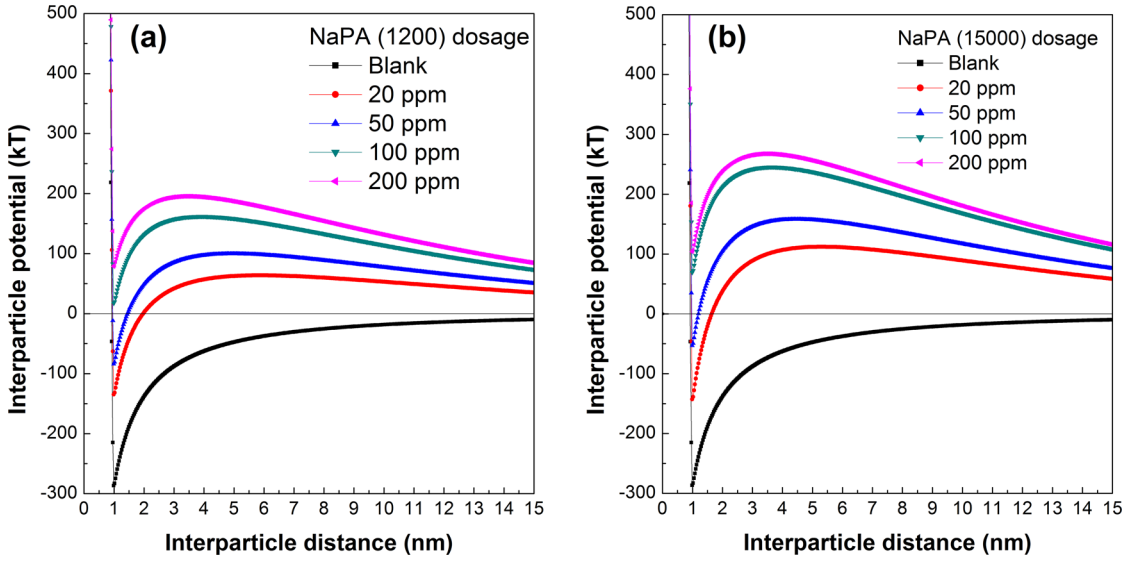

Figure 6. Interparticle potential calculations for the $Mg(OH)_2$ suspensions as a function of NaPA dosage. (a) NaPA (1200). (b) NaPA (15,000).

AUTHOR INFORMATION

Corresponding Authors

*Tel.: +86 21 64252170. Fax: +86 21 64250981. E-mail: xfsong@ecust.edu.cn (X.S.).
*Tel.: +86 21 64252170. Fax: +86 21 64250981. E-mail: jgyu@ecust.edu.cn (J.Y.).

Notes

The authors declare no competing financial interest.

REFERENCES

(1) Sada, E.; Kumazawa, H.; Sawada, Y.; Kondo, T. Simultaneous absorption of dilute nitric oxide and sulfur dioxide into aqueous slurries of magnesium hydroxide with added iron (II)-EDTA chelate. *Ind. Eng. Chem. Process Des. Dev.* **1982**, *21*, 771.
(2) Gui, H.; Zhang, X.; Dong, W.; Wang, Q.; Gao, J.; Song, Z.; Lai, J.; Liu, Y.; Huang, F.; Qiao, J. Flame retardant synergism of rubber and $Mg(OH)_2$ in EVA composites. *Polymer* **2007**, *48*, 2537.
(3) Cao, H.; Zheng, H.; Yin, J.; Lu, Y.; Wu, S.; Wu, X.; Li, B. $Mg(OH)_2$ complex nanostructures with superhydrophobicity and flame retardant effects. *J. Phys. Chem. C* **2010**, *114*, 17362.
(4) Martin, P. D.; Schneck, D. W.; Dane, A. L.; Warwick, M. J. The effect of a combination antacid preparation containing aluminium hydroxide and magnesium hydroxide on rosuvastatin pharmacokinetics. *Curr. Med. Res. Opin.* **2008**, *24*, 1231.
(5) Scott, G.; Reynolds, C. V.; Milosavljev, S.; Langholff, W.; Shenouda, M.; Rordorf, C. Lack of effect of omeprazole or of an aluminium hydroxide/magnesium hydroxide antacid on the pharmacokinetics of lumiracoxib. *Clin. Pharmacokinet.* **2004**, *43*, 341.
(6) Kang, J.; Schwendeman, S. P. Comparison of the effects of $Mg(OH)_2$ and sucrose on the stability of bovine serum albumin encapsulated in injectable poly(D,L-lactide-co-glycolide) implants. *Biomaterials* **2002**, *23*, 239.
(7) Tong, K.; Song, X.; Sun, S.; Xu, Y.; Yu, J. The rheological behavior and stability of $Mg(OH)_2$ aqueous suspensions in the presence of sodium polyacrylate. *Colloids Surf., A* **2013**, *436*, 1111.
(8) Lv, X.; Li, M.; Ma, X.; Ma, S.; Gao, Y.; Tang, L.; Zhao, J.; Guo, Y.; Zhao, X.; Wang, Z. In situ synthesis of nanolamellas of hydrophobic magnesium hydroxide. *Colloids Surf., A* **2007**, *296*, 97.
(9) Song, G.; Ma, S.; Tang, G.; Wang, X. Ultrasonic-assisted synthesis of hydrophobic magnesium hydroxide nanoparticles. *Colloids Surf., A* **2010**, *364*, 99.
(10) Ma, M. Enhancement of hematite flocculation in the hematite-starch-(low-molecular-weight) poly(acrylic acid) system. *Ind. Eng. Chem. Res.* **2011**, *50*, 11950.
(11) Palmqvist, L.; Holmberg, K. Dispersant adsorption and viscoelasticity of alumina suspensions measured by quartz crystal microbalance with dissipation monitoring and in situ dynamic rheology. *Langmuir* **2008**, *24*, 9989.
(12) Yokosawa, M. M.; Pandolfelli, V. C.; Frollini, E. Influence of pH and time on the stability of aqueous alumina suspensions containing sodium polyacrylates: A revisited process. *J. Dispersion Sci. Technol.* **2002**, *23*, 827.
(13) Cesarano, J., III; Aksay, I. A. Processing of highly concentrated aqueous α-alumina suspensions stabilized with polyelectrolytes. *J. Am. Ceram. Soc.* **1988**, *71*, 1062.
(14) Luo, Q. Stabilization of alumina polishing slurries using phosphonate dispersants. *Ind. Eng. Chem. Res.* **2000**, *39*, 3249.
(15) Wiśniewska, M.; Chibowski, S.; Urban, T. Adsorption and thermodynamic properties of the alumina-polyacrylic acid solution system. *J. Colloid Interface Sci.* **2009**, *334*, 146.
(16) Liufu, S.; Xiao, H.; Li, Y. Adsorption of poly(acrylic acid) onto the surface of titanium dioxide and the colloidal stability of aqueous suspension. *J. Colloid Interface Sci.* **2005**, *281*, 155.
(17) Chibowski, S.; Wiśniewska, M.; Urban, T. Influence of solution pH on stability of aluminum oxide suspension in presence of polyacrylic acid. *Adsorption* **2010**, *16*, 321.
(18) Studart, A. R.; Amstad, E.; Gauckler, L. J. Colloidal stabilization of nanoparticles in concentrated suspensions. *Langmuir* **2007**, *23*, 1081.
(19) Furusawa, K.; Ueda, M.; Nashima, T. Bridging and depletion flocculation of synthetic latices induced by polyelectrolytes. *Colloids Surf., A* **1999**, *153*, 575.
(20) Aschauer, U.; Burgos-Montes, O.; Moreno, R.; Bowen, P. Hamaker 2: A toolkit for the calculation of particle interactions and suspension stability and its application to mullite synthesis by colloidal methods. *J. Dispersion Sci. Technol.* **2011**, *32*, 470.
(21) Luckham, P. F.; Rossi, S. The colloidal and rheological properties of bentonite suspensions. *Adv. Colloid Interface Sci.* **1999**, *82*, 43.
(22) Hogg, R.; Healy, T.; Fuerstenau, D. Mutual coagulation of colloidal dispersions. *Trans. Faraday Soc.* **1966**, *62*, 1638.
(23) Ondaral, S.; Usta, M. Effects of dissolved organic compounds and electrolyte on precipitated calcium carbonate retention in papermaking. *Ind. Eng. Chem. Res.* **2010**, *49*, 12185.
(24) Rogan, K.; Bentham, A.; Beard, G.; George, I.; Skuse, D. Sodium polyacrylate mediated dispersion of calcite. *Prog. Colloid Polym. Sci.* **1994**, *97*, 97.

(25) Laarz, E.; Bergström, L. The effect of anionic polyelectrolytes on the properties of aqueous silicon nitride suspensions. *J. Eur. Ceram. Soc.* **2000**, *20*, 431.
(26) Rhodes, S. K.; Lambeth, R. H.; Gonzales, J.; Moore, J. S.; Lewis, J. A. Cationic comb polymer superdispersants for colloidal silica suspensions. *Langmuir* **2009**, *25*, 6787.
(27) Sun, J.; Bergström, L.; Gao, L. Effect of magnesium ions on the adsorption of poly(acrylic acid) onto alumina. *J. Am. Ceram. Soc.* **2001**, *84*, 2710.
(28) Tseng, W. J.; Tzeng, F. Effect of ammonium polyacrylate on dispersion and rheology of aqueous ITO nanoparticle colloids. *Colloids Surf., A* **2006**, *276*, 34.
(29) Sato, K.; Kondo, S.; Tsukada, M.; Ishigaki, T.; Kamiya, H. Influence of solid fraction on the optimum molecular weight of polymer dispersants in aqueous TiO_2 nanoparticle suspensions. *J. Am. Ceram. Soc.* **2007**, *90*, 3401.
(30) Sigmund, W. M.; Bell, N. S.; Bergström, L. Novel powder − Processing methods for advanced ceramics. *J. Am. Ceram. Soc.* **2000**, *83*, 1557.
(31) Lyckfeldt, O.; Palmqvist, L.; Carlström, E. Stabilization of alumina with polyelectrolyte and comb copolymer in solvent mixtures of water and alcohols. *J. Eur. Ceram. Soc.* **2009**, *29*, 1069.
(32) Palmqvist, L.; Lyckfeldt, O.; Carlström, E.; Davoust, P.; Kauppi, A.; Holmberg, K. Dispersion mechanisms in aqueous alumina suspensions at high solids loadings. *Colloids Surf., A* **2006**, *274*, 100.
(33) Lewis, J. A. Colloidal processing of ceramics. *J. Am. Ceram. Soc.* **2000**, *83*, 2341.
(34) Flatt, R. J.; Bowen, P. Yodel: A yield stress model for suspensions. *J. Am. Ceram. Soc.* **2006**, *89*, 1244.
(35) Flatt, R. J.; Bowen, P. Yield stress of multimodal powder suspensions: An extension of the YODEL (Yield Stress mODEL). *J. Am. Ceram. Soc.* **2007**, *90*, 1038.
(36) Tseng, W. J.; Lin, K.-C. Rheology and colloidal structure of aqueous TiO_2 nanoparticle suspensions. *Mater. Sci. Eng., A* **2003**, *355*, 186.
(37) Dimic-Misic, K.; Gane, P.; Paltakari, J. Micro-and nanofibrillated cellulose as a rheology modifier additive in CMC-containing pigment-coating formulations. *Ind. Eng. Chem. Res.* **2013**, *52*, 16066.
(38) Tseng, W. J.; Nian, J. Effect of ammonium polyacrylate on rheology of anatase TiO_2 nanoparticles dispersed in silicon alkoxide sols. *Ceram. Int.* **2004**, *30*, 2305.
(39) Albano, M. P.; Garrido, L. B. Rheological properties of Si_3N_4, pseudoboehmite and bayerite coated Si_3N_4 suspensions with ammonium polyacrylate dispersant. *Colloids Surf., A* **2002**, *203*, 117.
(40) Jean, J. H.; Wang, H. R. Effects of solids loading, pH, and polyelectrolyte addition on the stabilization of concentrated aqueous $BaTiO_3$ suspensions. *J. Am. Ceram. Soc.* **2000**, *83*, 277.
(41) Ghosh, S.; Jiang, W.; McClements, J. D.; Xing, B. Colloidal stability of magnetic iron oxide nanoparticles: Influence of natural organic matter and synthetic polyelectrolytes. *Langmuir* **2011**, *27*, 8036.
(42) Henrist, C.; Mathieu, J. P.; Vogels, C.; Rulmont, A.; Cloots, R. Morphological study of magnesium hydroxide nanoparticles precipitated in dilute aqueous solution. *J. Cryst. Growth* **2003**, *249*, 321.
(43) Şakar-Deliormanlı, A.; Celik, E.; Polat, M. Adsorption of anionic polyelectrolyte and comb polymers onto lead magnesium niobate. *Colloids Surf., A* **2008**, *316*, 202.
(44) Vermöhlen, K.; Lewandowski, H.; Narres, H.-D.; Schwuger, M. Adsorption of polyelectrolytes onto oxides-the influence of ionic strength, molar mass, and Ca^{2+} ions. *Colloids Surf., A* **2000**, *163*, 45.
(45) Kirby, G. H.; Lewis, J. A. Comb polymer architecture effects on the rheological property evolution of concentrated cement suspensions. *J. Am. Ceram. Soc.* **2004**, *87*, 1643.
(46) Flood, C.; Cosgrove, T.; Espidel, Y.; Howell, I.; Revell, P. Sodium polyacrylate adsorption onto anionic and cationic silica in the presence of salts. *Langmuir* **2007**, *23*, 6191.
(47) He, M.; Addai-Mensah, J.; Beattie, D. The influence of polymeric dispersants on sericite-chalcocite particle interactions in aqueous media. *Chem. Eng. J.* **2009**, *152*, 471.